

## THE INFLUENCE OF RESIDUAL STRESS FIELDS AND SHEET THICKNESS ON STRESS DISTRIBUTIONS IN RIVETED JOINT

Elżbieta Szymczyk

Military University of Technology  
Faculty of Mechanical Engineering, Department of Mechanics and Applied Computer Science  
Kaliskiego 2 Street, 00-908 Warsaw  
tel.: +48 022 683 90 39, fax: +48 022 683 94 61  
e-mail: eszymczyk@wat.edu.pl

### Abstract

Riveting is a traditional, but still popular (particularly in aviation) method of joining metal and composite elements. The residual stress and plastic strain states occur in the joint after the riveting process. The total stress experienced by the material at a given location within a component depends on the residual and applied stress. Residual post-riveting stress fields are widely accepted to have a significant influence on the fatigue life of aircraft structures. The single lap riveted joint consisting of two sheets and three rows of rivets are analysed. Two specimens are taken into consideration: sheet width and pitch distance are equal to 10.5 mm and rivet diameter is equal to 3.5 mm in the former case whereas 25 mm wide sheets and 5 mm rivet diameter are used in the later case. Distance between rivets (pitch length) and sheet width are equal to 3 or 5 rivet diameters. Materials used in riveted joints are subjected to plastic deformation. The rivet (PA24) and the sheet (2024T3) aluminium alloys are described using piecewise linear material models. The yield stress for the multiaxial state is calculated using the von Mises yield criterion. The paper deals with analysis of the pitch length and sheet thickness influence on stress fields. Stress concentrations around the holes in the rivet row and its distribution between rows are calculated. Models with and without residual stresses are taken into consideration. Local change of the sheet thickness causes a decrease in secondary bending of the joint. This is a result of a small increase in bending between the rivet rows and a simultaneous decrease in maximum bending stress values.

**Keywords:** riveted joint, residual stresses, secondary bending, FEM

### 1. Introduction

Aircraft structures, such as airplane or helicopter fuselages, wings etc. are thin-walled ones, with coverings made of thin sheets stiffened with stringers, frames or ribs. Sheets are typically assembled by multiple riveted or bolted joints. Rivets and bolts are also used to joint sheets and stiffeners. The riveted joints are critical areas of the aircraft structure due to severe stress concentrations, plastic strain, secondary bending and micro-local effects such as surface damage (fretting wear). These phenomena cause initiation and propagation of fatigue crack and decrease fatigue resistance of the riveted joint [1-4].

Fatigue performance of a riveted joint depends on structural, material and manufacturing factors. Among structural factors the following ones should be mentioned: type of the joint, its dimensions, sheet thickness, rivet diameter and type as well as distance between rivets and rivet rows (pitch length).

The paper deals with analysis of the pitch length and sheet thickness influence on stress fields. Stress concentrations around the holes in the rivet row and its distribution between rows are calculated. Models with and without residual stresses are taken into consideration.

### 2. Riveted specimens

The single lap riveted joints consisting of two sheets and three rows of rivets are considered (Fig. 1). Distance between rivets (pitch length) and sheet width are equal to 3 rivet diameters

(minimum pitch specified in manufacturing instruction) or 5 rivet diameters. The joint dimensions are given in Tab. 1.

Tab. 1. Joint dimensions in [mm]

case	sheet length	sheet width / pitch length	sheet thickness	rivet diameter
w1	170	10.5	1.2	3.5
w2	170	10.5	1.2	3.5
c1	210	25	2.0	5.0
c2	223	25 / 37.5	2.0 / 1.0	5.0

Two cases of initial conditions are taken into account in the first part of analysis. In case w1 residual stress fields are generated/created/set around the rivet holes [5] then the specimen is subjected to tensile load, whereas in case w2 specimen without residual stresses is considered. Some results for this specimen are presented in paper [5]. The continuation of those analyses is performed, especially the influence of residual stress fields (reminded after riveting process) on stress distribution in the rivet row (cross section N1) and between them (sheet cross sections A-A and B-B).

Then the analysis is carried out for two cases of riveted joint with different sheet thickness conditions [3]. The basic model c1 is described above. Case c2 (Fig. 2) is a result of a local change (milling) of the sheet thickness to 1 mm. Moreover, the mass of the joint remains the same as in case c1. Consequently (in case c2) the entire length of the sheet is 223 mm and the distance between rivet rows (pitch length) increases to 37.5 mm. Specimens without residual stresses are taken into consideration in this part of analysis.

Specimens are made of aluminium alloy 2024T3 used in aircraft structures whereas rivets are made of PA24 alloy. The following stress-strain curves (given in Fig. 3) are assumed in analysis.

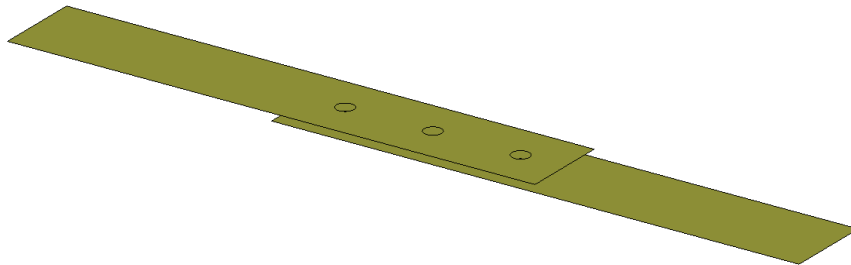


Fig. 1. Geometry of the specimen - case c1

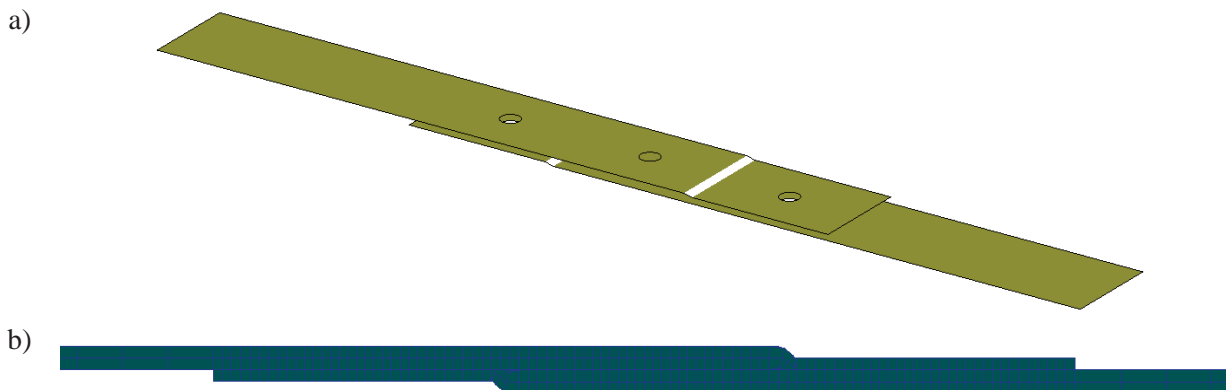


Fig. 2. Geometry of the specimen - case c2 a) axonometric view b) plane view

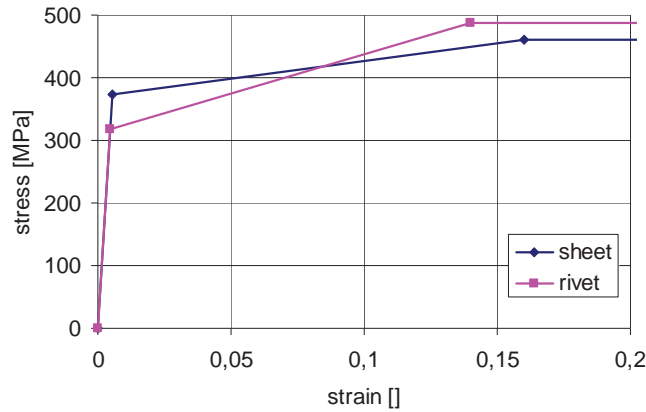


Fig. 3. Nonlinear stress – strain curve

### 3. Numerical models

Numerical models are prepared using MSC.Patran and calculations are carried out with MSC.Nastran and MSC.Marc codes. The sheet models consist of four-node, isoparametric, membrane-bending surface elements (type QUAD4) [6, 7]. Rounded mesh shape and small elements close to the rivet holes and larger elements a bit further from the rivet region are taken into account. The rivets and their interaction with the sheets are described using beam, shell and rigid elements as well as Gap node-to-node contact elements [6]. Sheet interaction is also modelled with Gap elements. Stiffness of contact elements equal to  $10^5$  N/mm corresponding to sheet stiffness (1) is assumed.

$$k = \frac{EA}{g}, \quad (1)$$

where:

E - Young modulus,

A - area of the element cross section,

g - sheet thickness around the rivet hole.

FE mesh of the sheet around the rivet holes is presented in Fig. 4. The model of riveted joint (case c1) and notation of rivet rows, sheet cross sections and sheet layers used in the paper are shown in Fig. 5.

A bilinear elasto-plastic sheet material model (Fig. 3) and linear elastic rivet material are used in calculations. The magnitude of the yield stress and tensile strength are obtained from an uniaxial test and the yield value for the multiaxial state is calculated using the von Mises criterion.

However grips of the testing machine are set in one plane (one above the other), the relative shift of the middle surfaces of upper and lower sheets is equal to 2 mm. Therefore initial displacement of the gripping tabs of the upper sheet is considered. Boundary conditions and two steps of the specimen loading are presented in Fig. 6.

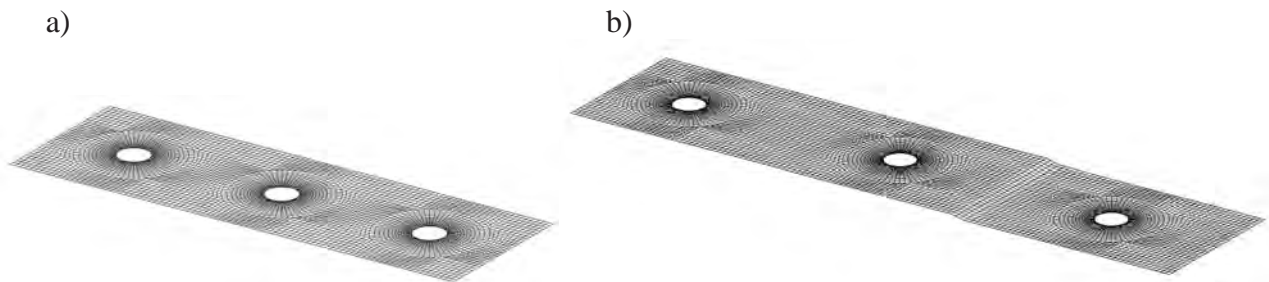


Fig. 4. Mesh of the sheet in the riveted region a) case c1, b) case c2

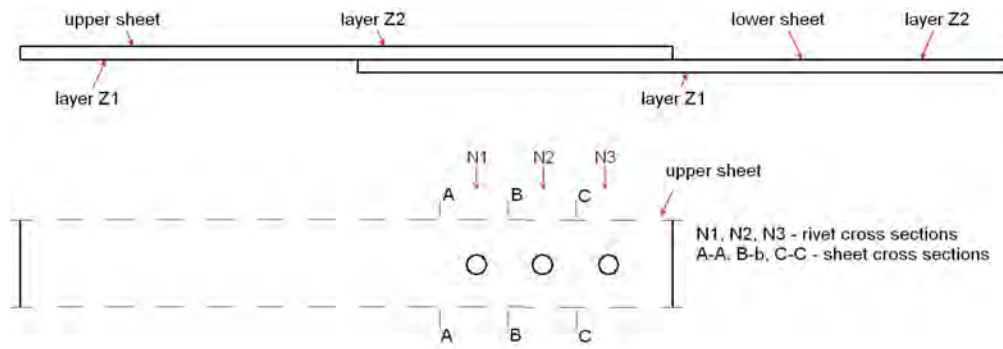


Fig. 5. Joint scheme

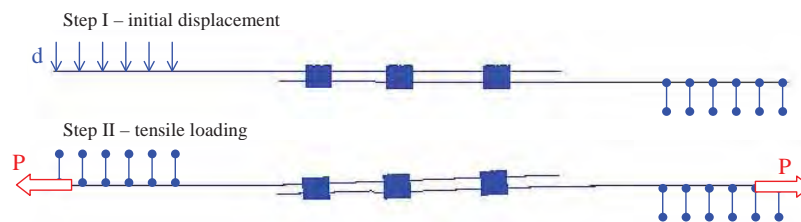


Fig. 6. Two steps of loading

#### 4. Numerical results

Tensile load corresponding to the stress level  $80 \text{ MPa}$  ( $0.214 \cdot R_e$ ) is applied. The stress distributions in sheet cross sections (A-A and B-B) and rivet row N1 are shown in Fig. 7 and 8 respectively. The results are presented in outer sheet layers Z1 and Z2 (Fig. 5) for upper sheet only due to point symmetry of the specimen.

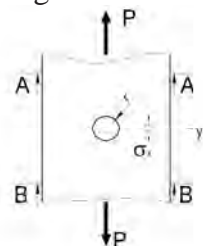
Secondary bending (stress value equal to  $0.35 \cdot R_e$ ) is recognised in case w2 in sheet cross section A-A (Fig. 7a) whereas stress distributions for layers Z1 and Z2 are nearly the same (there is no bending) in sheet cross section B-B (Fig. 7b).

The residual stress field has a significant influence on stress distribution in the specimen subjected to tensile loading. Residual stress distribution and distribution after tensile loading as well as difference between those stresses (which can be understood as a part of stresses caused/produced by tensile load) for case w1 are presented in sheet cross sections (Fig. 7 c-h).

Stress diagrams are similar in section A-A. The influence of residual stresses is more visible in section B-B (between the rivet rows): stress distribution after tensile loading is parallel to residual distribution therefore the difference is almost constant (Fig. 7 h). This is a result of the residual plastic strain field around the rivet holes.

Stress diagrams in rivet row N1 are presented in Fig. 8. Stress concentration occurs close to the rivet hole (Fig. 8a) in case w2, the bending stress value (in rivet row N1) close to the sheet edge is equal to  $0.23 R_e$ .

If a hole expansion is large enough, the compression stress field around the rivet hole remains after riveting process (Fig. 8b). Consequently, the stress concentration related to tensile loading occurs not at the rivet hole but a few millimetres further from the hole (Fig. 8c). Differences between stresses after tensile loading and after riveting under the rivet head are not regular (Fig. 8d).



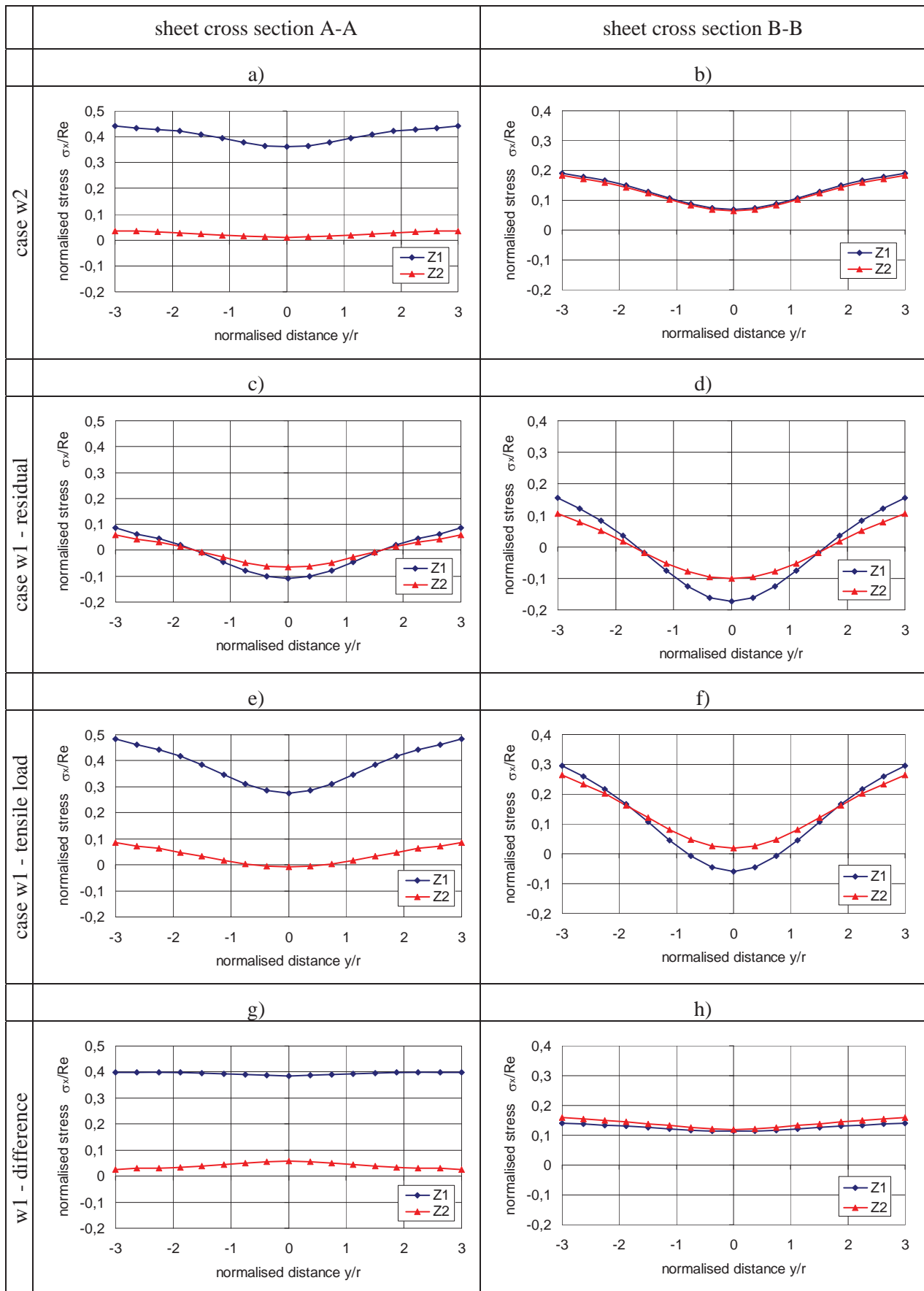


Fig. 7. Stress diagrams in sheet cross sections

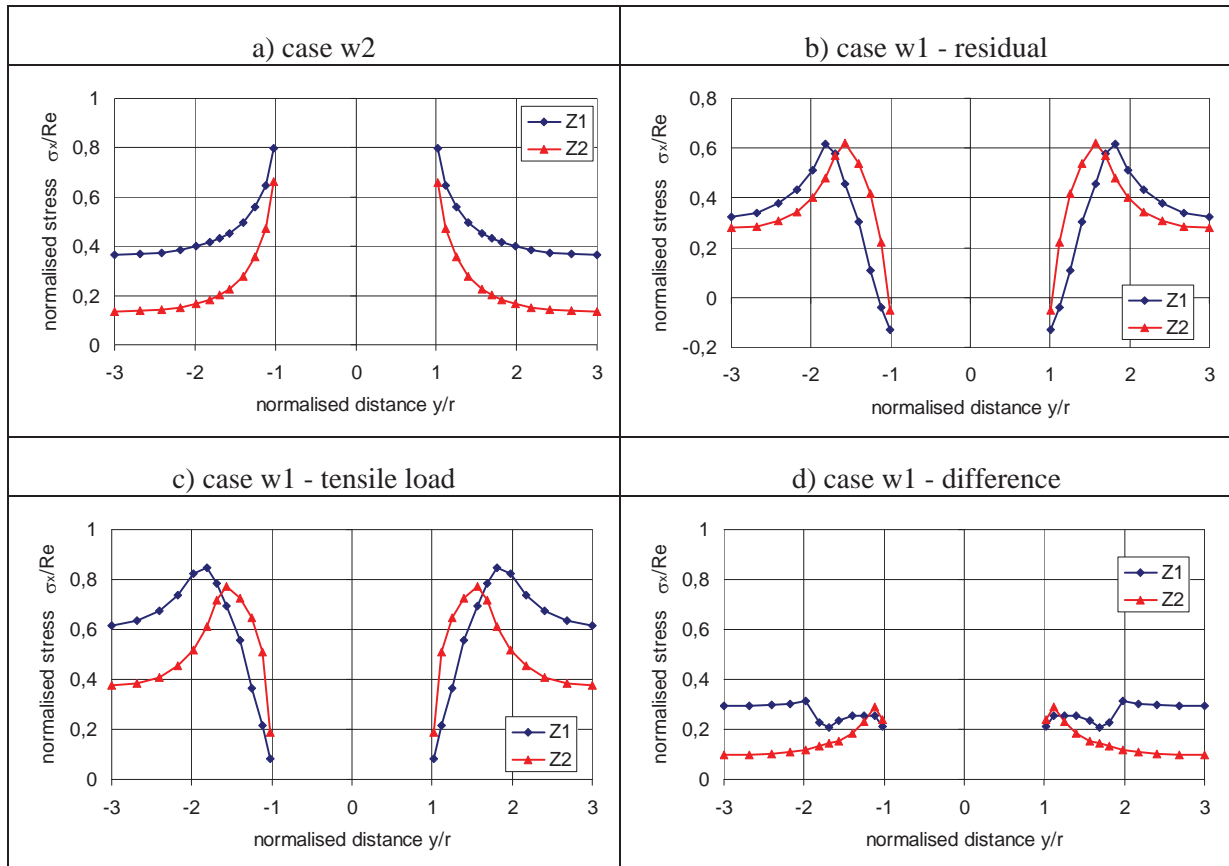


Fig. 8. Stress diagrams in cross sections N1

Secondary bending stresses are compared in Tab. 2. Residual stress field causes a slight increase in bending in section B-B and a simultaneous decrease in section A-A.

Tab. 2. Bending stresses

case	section A-A	section N1	section B-B
w1	$0.35 \cdot R_e$	$0.240 \cdot R_e$	$0.016 \cdot R_e$
w2	$0.38 \cdot R_e$	$0.230 \cdot R_e$	$0.005 \cdot R_e$

The second part of the paper deals with analysis of the sheet thickness influence on stress distributions and secondary bending of the specimen. Stress diagrams in the first rivet row (N1) for cases c1 and c2 are compared in Fig. 9 a-b. Stress distributions in cross sections A-A and B-B are presented in Fig. 9 c-d and e-f, respectively. Secondary bending is larger in section A-A (case c1) whereas in section B-B it is practically not recognised. In case c2 slight bending occurs in section B-B however it causes a decrease in bending stress in section A-A.

Secondary bending stress values are compared in Tab. 3.

Tab. 3. Bending stresses

case	section A-A	section N1	section B-B
c1	$0.26 \cdot R_e$	$0.140 \cdot R_e$	$0.005 \cdot R_e$
c2	$0.21 \cdot R_e$	$0.114 \cdot R_e$	$0.038 \cdot R_e$

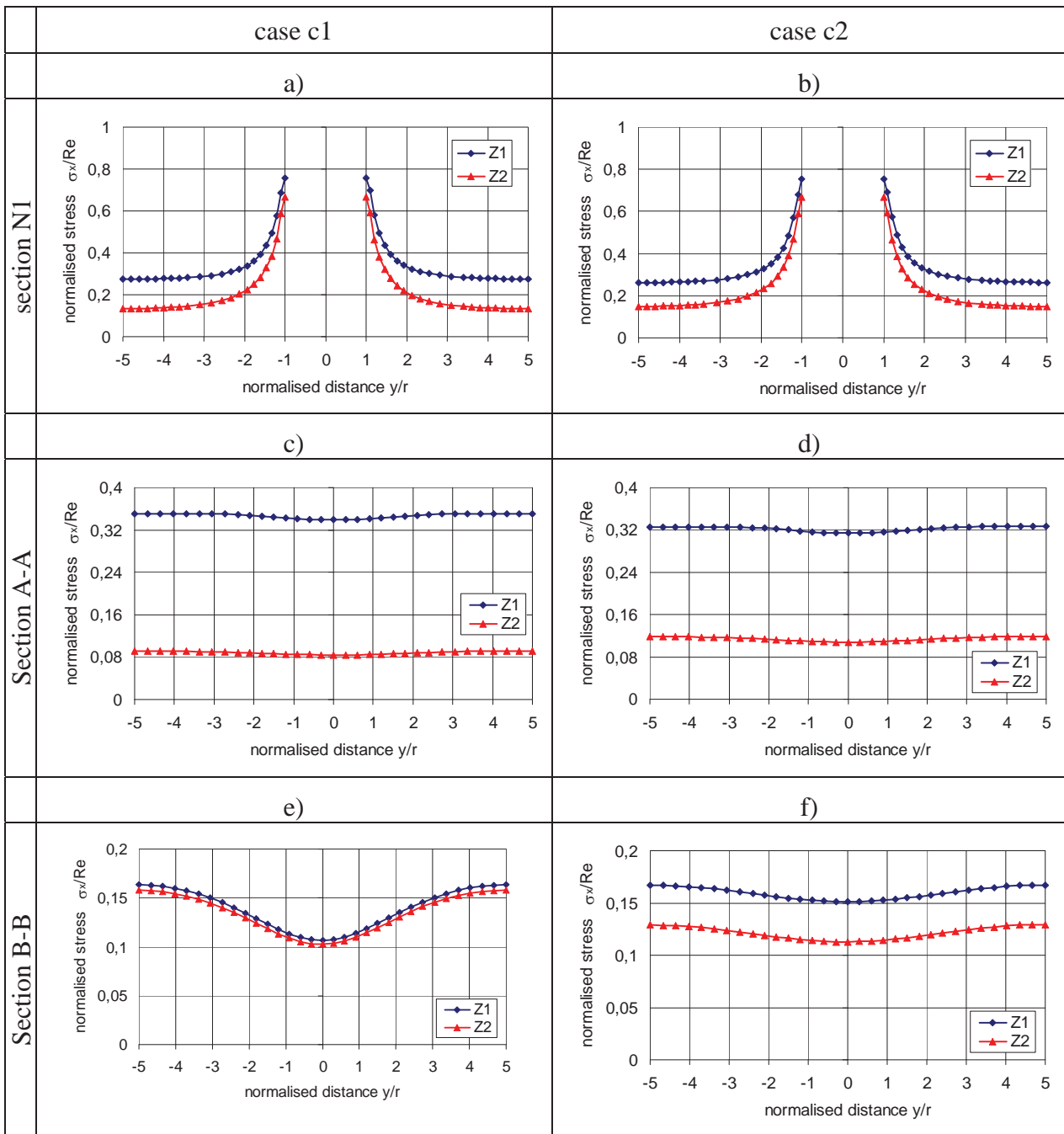


Fig. 9. Stress diagrams in cases c1 and c2

## 5. Summary

Structural and manufacturing factors have an effect on stress distributions in riveted joints. The influence of residual stresses and sheet thickness on secondary bending of the lap riveted joint are discussed in the paper.

The residual stress field has a significant influence on stress distribution in the specimen subjected to tensile loading. Stress concentration (related to tensile loading) occurs at the rivet hole if residual stresses are not taken into account, while the consideration of residual stresses causes that it takes place a few millimetres (about half a rivet radius) from the hole. Consequently, fatigue crack path doesn't go ahead exactly in the rivet row but around the rivet holes [1, 2].

In section B-B (between the rivet rows) stress distribution after tensile loading is parallel to

residual distribution therefore the difference is almost constant. However, actual stresses are smaller behind the rivet and larger close to the sheet edge.

The local change of the sheet thickness causes a decrease in secondary bending of the joint. This is a result of small increase in bending between the rivet rows and a simultaneous decrease in maximum bending stress values. The improvement of fatigue performance of the joint due to the local change of the sheet is reported in paper [3].

## References

- [1] de Rijck, J., *Stress Analysis of Fatigue Crack in Mechanically Fastened Joints*, Doc. Dissertation, Delft University of Technology, 2005.
- [2] Rans, C. D., *The Role of Rivet Installation on the Fatigue Performance of Riveted Lap Joints*, Doctoral Dissertation, Department of Mechanical and Aerospace Engineering Carleton University, 2007.
- [3] Skorupa, M., Skorupa, A., Machniewicz, T., Korbel, A., *An experimental investigation on the fatigue performance of riveted lap joints*, 25th Symposium of the International Committee on Aeronautical Fatigue (ICAF 2009), Rotterdam 2009.
- [4] Kaniowski, J., Wronicz, W., Jachimowicz, J., Szymczyk, E., *Methods for FEM analysis of riveted joints of thin-walled aircraft structures within the IMPERJA Project*, 25th Symposium of the International Committee on Aeronautical Fatigue (ICAF 2009), Rotterdam 2009.
- [5] Szymczyk, E., Jachimowicz, J., Sławiński, G., *Global approach in modelling of riveted joints*, 9th International Conference - Shell Structures, Theory and Applications, Jurata 2009.
- [6] MSC.Marc Theoretical Manual, MSC Corp. 2007.
- [7] MSC.Nastran Quick Reference Guide, MSC Corp. 2005.

## Acknowledgements

This work was carried out with the financial support of Polish Ministry of Science and Higher Education under research project in the framework of the Eureka Initiative.